2013 European Control Conference (ECC)
July 17-19, 2013, Zürich, Switzerland.

Experimental Validation of Interval-Based Sliding Mode Control for Solid Oxide Fuel Cell Systems

Thomas Dötschel, Andreas Rauh, Luise Senkel, and Harald Aschemann

Abstract— **The utilization of solid oxide fuel cells (SOFCs) as well as other high-temperature fuel cells for a decentralized power supply demands for reliable and guaranteed stabilizing control strategies, that are capable of providing electrical and thermal energy. Moreover, it is essential to increase the number of possible thermal cycles of SOFCs by means of control laws which reduce temperature gradients in the space coordinates of a stack module during transient operating conditions. For this purpose, suitable control-oriented system models have been identified in previous work and parameterized reliably by means of both local and global optimization procedures. By exploiting these models, which can be extended to account for parameters that are subject to bounded uncertainty, interval-based sliding mode controllers can be derived. These controllers simultaneously adjust the mass flow and temperature of air supplied to the cathode of the SOFC. In this paper, a real-time capable implementation of the corresponding interval-based sliding mode controller and selected experimental results are presented for an SOFC test rig available at the Chair of Mechatronics at the University of Rostock.**

Index Terms— **Control applications, energy systems, interval methods, sliding mode control, disturbance estimation**

I. Introduction

SOFC systems are characterized by their capability to operate at high temperatures. This leads to a high overall efficiency and to the possibility to use different fuel gases such as pure hydrogen and natural gas. Furthermore, SOFCs can be applied as decentralized energy supply systems that provide both process heat and electricity. For basic information concerning the fuel cell technology, the reader is referred to [1], [6], [12]. To implement automatized operating strategies for such energy supply devices, suitable model-based control procedures are required that are capable of working in wide operating ranges, see [5], [8].

An SOFC stack typically consists of a series connection of individual fuel cell elements. The stack module is the principal component if thermodynamic and electrochemical phenomena are considered. By using the first law of thermodynamics, a relation between the dominant influence factors on the internal energy and the overall temperature of the SOFC stack module can be derived. These influences are characterized by the enthalpy flows of both the preheated fuel gas and air, the thermal heat flow through the insulation of the stack module as well as the reaction heat flow and the internal heat conduction of the stack module. The number of influence factors increases if an electrical load is connected to the system. This leads to the conduction of oxygen ions from the cathode through the electrolyte to the anode, which further results in Ohmic losses. Additionally, the reduction of oxygen at the cathode and the oxidation of hydrogen at the anode have to be enabled. Furthermore, the electrochemical reaction in each fuel cell element is characterized by the production of water vapor at the anodes. These processes contribute to an increase of the internal energy of the stack due to their corresponding exothermic reaction enthalpy. In the case of using natural gas instead of pure hydrogen as a fuel gas, the overall reaction enthalpy is reduced by the preceding endothermic reforming reactions.

To obtain suitable control laws, it is essential to derive a system model consisting of a set of ordinary differential equations (ODEs). Here, the most dominant physical phenomena are included in the mathematical model of the SOFC stack. The system representation that is used in this paper results from a global energy balance over the complete stack module, leading to a scalar ODE for a single lumped temperature variable, cf. [8].

A further refinement of the mathematical model can be achieved by a semi-discretization of the stack module into finite volume elements in order to approximate the space dependency of the temperature profile, see [4], [5], [9]. The prerequisite for this approach is that the energy conservation law holds for each finite volume element in an integral sense. In analogy to the before-mentioned case, an ODE is derived for each finite volume element that is coupled with the ODEs of all neighboring elements. In such a way, infinite-dimensional descriptions commonly given by sets of nonlinear partial differential equations are replaced by finite-dimensional sets of ODEs.

In this paper, the nonlinear, guaranteed stabilizing control design is restricted to a scalar system model. For this system model, a novel interval-based sliding mode controller is employed to account for bounded uncertainty of the parameters characterizing the dynamic behavior of the thermal subsystem and to account for disturbance variables estimated in real time. The presented system description can also be generalized to higher dimensions, see [5], [9].

This paper is structured as follows: In Sec. II, an overview of fundamental modeling techniques for the thermal behavior of SOFC systems is given. Sec. III describes an approach for the stabilization of the thermal behavior of the SOFC stack module by using an interval-based sliding mode control law which is extended by an online disturbance compensation. The disturbance to be compensated is estimated by means of an observer which exploits the nonlinear lumped parameter

A. Rauh, L. Senkel, and H. Aschemann are with the Chair of Mechatronics, University of Rostock, Justus-von-Liebig-Weg 6, D-18059 Rostock, Germany {Andreas.Rauh, Luise.Senkel, Harald.Aschemann}@uni-rostock.de

Th. Dötschel was with the same institute while this work was performed.

model of the thermal subsystem. Experimental results are presented in Sec. III-D to validate the practical applicability of the control approach. Finally, conclusions and an outlook on future work are given in Sec. IV.

II. Modeling of the Thermal Behavior of SOFCs

To design suitable control strategies for the non-stationary operation of SOFC systems, a nonlinear mathematical system model is used. This model is based on an integral formulation of the first law of thermodynamics. The non-stationary behavior results from variations of the internal energy of the system which are related to variations of the internal temperature. In detail, the internal energy of SOFC stack modules is affected by enthalpy flows of both the fuel gas and air as well as by heat conduction between the individual fuel cell stack elements which are electrically connected in series.

If the overall exothermic chemical reaction

$$\begin{aligned} 2\ H_2 + 2O^{2-} &\rightarrow 2\ H_2O + 4e^- \quad \text{with} \\ O_2 + 4e^- &\rightarrow 2O^{2-} \end{aligned} \tag{1}$$

in a fuel cell element is enabled via an external electric current and ion conduction in the interior of the stack, the SOFC temperature additionally depends on the Ohmic losses of the fuel cell material as well as on the reaction enthalpy which is strongly affected by the choice of the fuel gas.

As a fundamental model, the thermal behavior can be described by a global energy balance. This leads to a scalar ODE for the temperature of the SOFC stack. This mathematical model cannot represent temperature gradients with respect to the space coordinates of the SOFC stack during non-stationary operating phases. This problem can be solved by a spatial semi-discretization leading to a set of coupled ODEs for the complete stack module. A detailed derivation of such control-oriented models can be found in [4], [8], [9] and the references therein. Disturbances as well as approximation errors of the finite-dimensional description of the original distributed parameter system can be quantified by observer techniques similar to those published in [7], [10].

A. Thermal Behavior of the SOFC Stack Module

A first modeling approach for the temperature ϑ_{FC} of the SOFC stack is based on the introduction of a single finite volume element. The energy flows passing the system boundary result in variations of the internal energy of the corresponding volume element. This element is defined in such a way that the thermal insulation of the SOFC stack is included within the system boundary according to Fig. 1.

Here, the variation $\dot{E}_{FC}$ of the internal energy is given by

$$\begin{aligned} \dot{E}_{FC}(t) = {} & C_{AG}(\vartheta_{FC}, t) \cdot (\vartheta_{AG,in}(t) - \vartheta_{AG,out}(t)) \\ & + C_{CG}(\vartheta_{FC}, t) \cdot (\vartheta_{CG,in}(t) - \vartheta_{CG,out}(t)) \\ & + \dot{Q}_R(t) + P_{El}(t) + \dot{Q}_A(t)\ , \end{aligned} \tag{2}$$

where $\vartheta_{FC} = \vartheta_{AG,out} = \vartheta_{CG,out}$ is commonly assumed. The heat flow $\dot{Q}_A$ through the thermal insulation of the stack

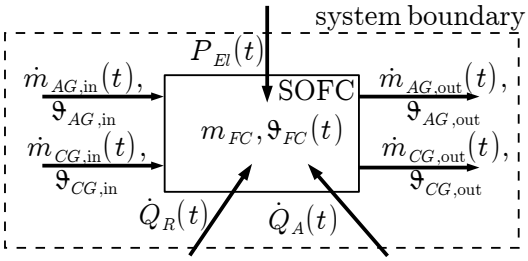

Fig. 1: Global energy balance for a fuel cell module (AG: anode gas; CG: cathode gas; FC: fuel cell).

module is described by

$$\dot{Q}_A(t) = \frac{1}{R_{th,A}} \cdot \Big(\vartheta_A - \vartheta_{FC}(t)\Big) \tag{3}$$

with the thermal resistance $R_{th,A}$ of the insulation and the ambient temperature ϑ_A. To simplify the mathematical model, heat radiation is included in this expression in a locally linearized manner leading to modeling errors in the case that high stack temperatures occur. For this reason as well as to account for non-negligible external disturbances, an observer approach is presented in Sec. III-A to estimate such model deviations.

The impact of electrochemical processes is determined by $P_{El}(t) = R_{El} \cdot I(t)^2$ which represents the heat flow due to Ohmic losses, resulting from the conduction of charge carriers in the fuel cell. Moreover, the reaction heat flow

$$\begin{aligned} \dot{Q}_R(t) &= \Delta_R H(\vartheta_{FC}) \cdot \dot{n}_{el}(t) \\ &= \Delta_R H(\vartheta_{FC}) \cdot \frac{I(t)}{z \cdot F}\ , \quad \dot{n}_{el}(t) = \frac{\dot{m}^R_{H_2}(t)}{M_{H_2}} \end{aligned} \tag{4}$$

with the mass flow of hydrogen $\dot{m}^R_{H_2}$ (consumed in the electrochemical reaction), its molar mass M_{H_2} as well as the electric current $I(t)$ is taken into account. The processes in (1) and (4) become relevant in the case of connecting an electrical load to the SOFC stack module, where the maximum current $I(t)$ between the electrodes is restricted by the consumed amount of hydrogen $\dot{m}^R_{H_2}$. This behavior is expressed by Faraday's law $I = z \cdot F \cdot \dot{n}_{el}$ with the Faraday constant F as well as the number of electrons z which participate in each reaction (1).

The enthalpy flow in Eq. (2) contains the heat capacity of the anode gas mixture according to

$$\begin{aligned} C_{AG}(\vartheta_{FC}, t) = {} & c_{H_2}(\vartheta_{FC}) \cdot \dot{m}_{H_2}(t) \\ & + c_{N_2}(\vartheta_{FC}) \cdot \dot{m}_{N_2}(t) + c_{H_2O}(\vartheta_{FC}) \cdot \dot{m}_{H_2O}(t)\ . \end{aligned} \tag{5}$$

The heat capacity for the cathode gas is given by

$$C_{CG}(\vartheta_{FC}, t) = c_{CG}(\vartheta_{FC}) \cdot \dot{m}_{CG}(t) \tag{6}$$

with the mass flow $\dot{m}_{CG}(t)$ of air and the specific heat capacity $c_{CG}(\vartheta_{FC})$. The specific heat capacities of hydrogen $c_{H_2}(\vartheta_{FC})$, nitrogen $c_{N_2}(\vartheta_{FC})$, water vapor $c_{H_2O}(\vartheta_{FC})$ and air $c_{CG}(\vartheta_{FC})$ are approximated by second-order polynomials

$$c_\chi(\vartheta_{FC}) = \sum_{i=0}^{2} \alpha_{\chi,i} \cdot \vartheta^i_{FC}\ . \tag{7}$$

The index $\chi \in \{H_2, N_2, H_2O, CG\}$ refers to each gas fraction. In the considered SOFC, the fuel gas mixture consists of hydrogen (supplied mass flow $\dot{m}_{H_2} \geq \dot{m}_{H_2}^R$), water vapor (mass flow $\dot{m}_{H_2O}$), and nitrogen (mass flow $\dot{m}_{N_2}$). The fuel gas and the air mass flow $\dot{m}_{CG}$ are preheated separately before they are supplied to the SOFC stack. Finally, the reaction enthalpy $\Delta_R H(\vartheta_{FC})$ is approximated by a second-order polynomial. Its coefficients as well as the parameters in (7) can be identified experimentally, see e.g. [4], [8], [10].

The variation of the internal energy $\dot{E}_{FC}(t)$ is related to the fuel cell temperature ϑ_{FC} by

$$\dot{\vartheta}_{FC}(t) = \frac{1}{c_{FC}\ m_{FC}} \dot{E}_{FC}(t) \tag{8}$$

in which the specific heat capacity c_{FC} and the mass m_{FC} characterize material parameters of the stack module.

B. Structural Analysis of the System Model

To design a robust sliding mode control strategy, the scalar SOFC model can be transformed exactly into the input-affine nonlinear ODE

$$\begin{aligned} \dot{\vartheta}_{FC} =& f(\vartheta_{FC}(t), \mathbf{p}, d, v(t)) \\ =& a\left(\vartheta_{FC}(t), \mathbf{p}, d\right) + b\left(\vartheta_{FC}(t), \mathbf{p}, d\right) \cdot v(t) \end{aligned} \tag{9}$$

with the interval parameter vector $\mathbf{p} \in [\mathbf{p}] = \left[\underline{\mathbf{p}}\ ;\ \overline{\mathbf{p}}\right]$, $\mathbf{p} \in \mathbb{R}^{n_p}$, and the disturbance $d \in [d] = \left[\underline{d}\ ;\ \overline{d}\right]$, $d \in \mathbb{R}$, with $\underline{d} \leq \overline{d}$. Moreover, the relation $\underline{\mathbf{p}} \leq \overline{\mathbf{p}}$ holds component-wise. In addition, the term b is chosen in such a way that the property $b\left(\vartheta_{FC}(t), \mathbf{p}, d\right) > 0$ is guaranteed despite uncertainties in $\mathbf{p}$ and d. In the case of a scalar system model, Eq. (9) contains the expressions

$$\begin{aligned} & a\left(\vartheta_{FC}, \mathbf{p}, d\right) = \\ & \frac{C_{AG}(\vartheta_{FC}, t) \cdot (\vartheta_{AG} - \vartheta_{FC})}{c_{FC}\ m_{FC}} + \frac{(\vartheta_A - \vartheta_{FC})}{c_{FC}\ m_{FC}\ R_{th,A}} \\ & + \frac{\Delta_R H(\vartheta_{FC})}{c_{FC}\ m_{FC}\ z\ F} I + \frac{R_{El}}{c_{FC}\ m_{FC}} I^2 + d \end{aligned} \tag{10}$$

with the additive disturbance d and

$$b\left(\vartheta_{FC}, \mathbf{p}, d\right) = \frac{c_{CG}}{c_{FC}\ m_{FC}}\ , \tag{11}$$

respectively.

The system input $v(t)$ directly results in a modification of the cathode gas enthalpy flow according to

$$v(t) = \dot{m}_{CG}(t) \cdot (\vartheta_{CG}(t) - \vartheta_{FC}(t))\ . \tag{12}$$

In (10), the additive disturbance d is estimated by a disturbance observer to compensate modeling errors caused by the before-mentioned simplifications. Using the corresponding estimated values, their influence can be counteracted by the control law that is described in Sec. III-B.

To deal with imperfect system knowledge, the parameters of the ODE (9) can be identified as bounded intervals to account for their uncertainty. This uncertainty basically results from the fact that specific system parameters in the interior of the stack module such as the heat capacities or the thermal resistances are not directly accessible for measurements in an experiment. In [4], [9], an optimization procedure has been presented for the detection of guaranteed enclosures for the system parameters.

In the following section, a robust control law is described for the stabilization of the thermal behavior of the stack module based on the scalar ODE in (9) containing (10), (11).

III. Robust Control Design

As a controlled variable, the stack temperature is considered which is assumed to be identical to the temperature of the exhaust gases according to the lumped parameter model. This assumption is consistent with the integral form of the first law of thermodynamics.

To design robust model-based control strategies for the non-stationary operation of the fuel cell system that include heat-up processes, cooling phases as well as the influence of load variations, a suitable set of system parameters has to be determined beforehand. The robustness of the mathematical model can be improved if imperfect system knowledge resulting from the space discretization and a model for inaccuracies of the measured quantities are taken into account by an identification of bounded intervals for all parameters. On the basis of a practically motivated choice of initial values, a C++ routine has been employed in previous work to perform a reliable offline parameter identification, see [9]. This procedure relies on subdivision strategies for the interval parameters and searches for a globally optimal parameterization of the model (9) with (10), (11).

Even though the parameter ranges can be quite wide, reliable control laws can be derived for uncertain system models. To guarantee asymptotic stability, an interval-based sliding mode controller is proposed in the following to account for the uncertain parameters as well as for estimates of bounded disturbances in a reliable way. The non-stationary control law allows for a disturbance rejection which is an important property for the application in decentralized power supply systems. Note, that this control design can also be performed if the global optimization routine in [9] fails to determine parameter ranges that are guaranteed to be admissible with respect to the model and its measurement tolerances. In such cases, the accuracy of the system model is guaranteed not to be worse than the one of the floating-point based parameterization determined by means of local optimization procedures [4].

A. Observer-Based Control Strategy

In the following, control parameterizations have to be avoided which lead to inacceptably slow dynamics due to estimates for parameters and disturbances which are too conservative. Hence, it is essential to apply techniques that are capable of estimating model errors during the operation of the plant in real time. This demand can be achieved by an observer approach that reconstructs model errors resulting from the simplifications that are made in Sec. II-A based on the measurement of the stack module temperature.

The values which are reconstructed by the disturbance observer represent the estimated stack module temperature

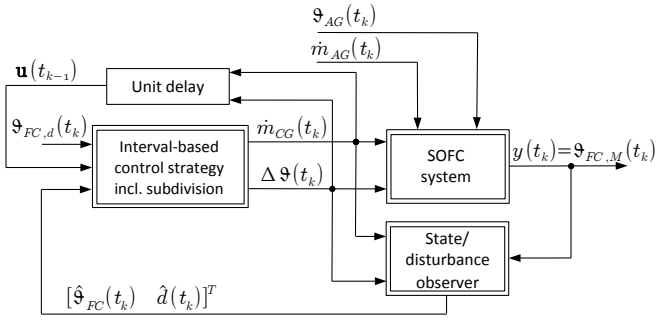

Fig. 2: Observer-based sliding mode control with an online estimation of modeling errors for the improvement of the control performance.

$\hat{\vartheta}_{FC}$ and the disturbance $\hat{d}$. For that purpose, the ODE of the thermal subsystem (9) with (10), (11) is extended to the observer equation

$$\frac{\mathrm{d}}{\mathrm{d}t}\begin{bmatrix}\hat{\vartheta}_{FC}\\ \hat{d}\end{bmatrix} = \begin{bmatrix} a\left(\hat{\vartheta}_{FC},\mathbf{p},\hat{d}\right)+b\left(\hat{\vartheta}_{FC},\mathbf{p},\hat{d}\right)\cdot v \\ 0\end{bmatrix} + \begin{bmatrix}K_1\\K_2\end{bmatrix}\cdot\Delta y \tag{13}$$

with the new state vector $\mathbf{x}_e^T = \begin{bmatrix}\hat{\vartheta}_{FC} & \hat{d}\end{bmatrix}$ and the output error $\Delta y = \left(\vartheta_{FC,M} - \hat{\vartheta}_{FC}\right)$ describing the deviation between the measured and estimated stack temperatures $\vartheta_{FC,M}$ and $\hat{\vartheta}_{FC}$, respectively. The observer parameters K_1 and K_2 are determined in such a way that the error dynamics of the observer (13) is stabilized asymptotically in a local manner despite disturbances acting on the thermal system. This is done by pole placement on the basis of a linearization of the nonlinear ODE (9) with respect to the state vector $\mathbf{x}_e$ in the current operating point. The pole placement is performed in such a way that the time constants for the observer structure are larger than the time constants of the thermal behavior of the stack module.

In Fig. 2, an observer-based control scheme is depicted which relies, on the one hand, on a feedback of the stack module temperature $y = \vartheta_{FC,M}$ and, on the other hand, on an estimation of the point-valued disturbance d, see also (13). To enhance robustness, the point-valued output $\hat{d}$ of the disturbance observer is converted into an interval variable before supplying it to the controller. It is assumed that the true disturbance value is enclosed by a lower bound $\underline{d} = \hat{d} - \Delta d$ and by an upper bound $\overline{d} = \hat{d} + \Delta d$, with the tolerance bound $\Delta d > 0$, in an interval-based disturbance expression $d \in \left[\underline{d}\,;\,\overline{d}\right]$ as presented in Sec. III-B.

B. Robust Sliding Mode Controller

For the design of a robust model-based controller, the uncertain system model in (9) with (10), (11) is taken into account. The improved parameter values determined by the routines described in [9] lead to the possibility to reduce switching amplitudes of the variable structure part of the sliding mode controller as far as possible. The most important properties of this controller are its capability to stabilize the system dynamics in a desired operating point in a guaranteed way as well as the rejection of disturbances acting on the system. To account for uncertainties in the system representation (9), the parameters $\mathbf{p} \in [\mathbf{p}]$ and the disturbances $d \in [d]$ are chosen from bounded intervals. In [5], the above-mentioned control procedure is generalized for higher-dimensional SOFC models with the differentially flat output as the controlled variable.

On the basis of Eq. (9), a sliding mode control law can be designed for tracking of a desired temperature profile $\vartheta_{FC,d}(t)$ for all possible bounded parameters $\mathbf{p} \in [\mathbf{p}]$ and disturbances $d \in [d]$. For the stabilization of the desired trajectory $\vartheta_{FC,d}(t)$, the Lyapunov function candidate

$$V\left(s(t)\right) = \frac{1}{2}s(t)^2 > 0 \tag{14}$$

is employed with the error measure $s(t) = \vartheta_{FC}(t) - \vartheta_{FC,d}(t)$ which defines the sliding surface $s(t) = 0$ in (9). The time derivative of (14) is given by

$$\dot{V}\left(s(t)\right) = s(t)\cdot\dot{s}(t) \ . \tag{15}$$

Its negative definiteness and thus the asymptotic stability of the closed-loop system can be guaranteed by choosing

$$\dot{V}\left(s(t)\right) \leq -\eta\cdot|s(t)| \tag{16}$$

for a strictly positive design parameter $\eta > 0$. To guarantee asymptotically stable convergence to $s(t) = 0$, the absolute value $|s(t)| = s(t)\cdot\mathrm{sign}\{s(t)\}$ of the error measure is substituted in (16). With the choice

$$\dot{s} + \eta\cdot\mathrm{sign}\{s\} = -\beta\cdot\mathrm{sign}\{s\} \ , \quad \beta > 0 \ , \tag{17}$$

the control law can be obtained from

$$\dot{s} + \underbrace{(\eta+\beta)}_{\tilde{\eta}}\cdot\mathrm{sign}\{s\} = 0 \ , \tag{18}$$

where $\tilde{\eta} > 0$ can be used to influence the convergence rate to $s(t) = 0$ and simultaneously to affect the control amplitudes. For a desired operating point $\vartheta_{FC,d} = \mathrm{const}$, the time derivative of the error measure is given by

$$\dot{s} = \dot{\vartheta}_{FC} = a\left(\vartheta_{FC}(t),\mathbf{p},d\right) + b\left(\vartheta_{FC}(t),\mathbf{p},d\right)\cdot v(t) \ , \tag{19}$$

where $v(t)$ serves as the control variable according to Eq. (9). The corresponding variable-structure control law

$$[v] := -\frac{a\left(\vartheta_{FC}(t),[\mathbf{p}],[d]\right)}{b\left(\vartheta_{FC}(t),[\mathbf{p}],[d]\right)} - \frac{\tilde{\eta}\cdot\mathrm{sign}\left(\vartheta_{FC}(t)-\vartheta_{FC,d}\right)}{b\left(\vartheta_{FC}(t),[\mathbf{p}],[d]\right)} \ , \tag{20}$$

evaluated for all possible uncertainties, stabilizes the thermal SOFC system described by the ODE (9) in a guaranteed way. Obviously, the evaluation of (20) by means of interval arithmetics [2] results in an interval-based, stabilizing control $[v]$. To implement the controller on the available test rig, floating-point values have to be chosen from (20) which fulfill the sign condition (16). For that reason, the following cases

$$v := \begin{cases}\sup\{[v]\} & \text{for} \quad s(t) \geq 0\\ \inf\{[v]\} & \text{for} \quad s(t) < 0\end{cases} \tag{21}$$

are distinguished depending on the sign of $s(t)$, where $s(t)$ is evaluated for the measured temperature values.

C. Subdivision Strategy for the Real-Time Implementation of the Control Law

A subdivision strategy is employed to determine appropriate control inputs $\dot{m}_{CG}$ and $\Delta\vartheta$ corresponding to the bounds (21) of the interval-based controller output $[v(t)]$. The vector of the control inputs for the SOFC system is defined as

$$\mathbf{u}(t) := \begin{bmatrix} \dot{m}_{CG}(t) & \Delta\vartheta(t) \end{bmatrix}^T \tag{22}$$

according to Fig. 2. The product of both the mass flow $\dot{m}_{CG}(t)$ and the temperature difference $\Delta\vartheta(t) = \vartheta_{CG}(t) - \vartheta_{FC}(t)$ defines the system input according to

$$v(t_k) := \dot{m}_{CG}(t_k) \cdot \Delta\vartheta(t_k) \ , \tag{23}$$

which is computed at discrete points of time $t = t_k$.

A *validity* test of $\left[v^{<l>}\right] = \left[\dot{m}_{CG}^{<l>}\right] \cdot \left[\Delta\vartheta^{<l>}\right]$ is performed according to the controller output $[v]$ in (20) for classifying (i) *guaranteed consistent*, (ii) *undecided*, and (iii) *guaranteed inconsistent* input intervals.

For this classification, the system input vector $[\mathbf{u}]$ is initialized with $\left[\dot{m}_{CG}^{<ini>}\right]$ and $\left[\Delta\vartheta^{<ini>}\right]$, where the lower and upper interval bounds enclose the complete operating range of the mass flow controller as well as the preheater for the cathode gas. This interval box is subdivided further into 4 intervals by an element-wise bisectioning of the vector $\left[\mathbf{u}^{<l>}\right]$ according to

$$\begin{bmatrix} [\dot{m}_{CG}^{<l>}] \\ [\Delta\vartheta^{<l>}] \end{bmatrix} := \begin{bmatrix} \left[\inf\left([\dot{m}_{CG}^{<l>}]\right) \ ; \ \mathrm{mid}\left([\dot{m}_{CG}^{<l>}]\right)\right] \\ \left[\inf\left([\Delta\vartheta^{<l>}]\right) \ ; \ \mathrm{mid}\left([\Delta\vartheta^{<l>}]\right)\right] \end{bmatrix},$$

$$\begin{bmatrix} [\dot{m}_{CG}^{<L+1>}] \\ [\Delta\vartheta^{<L+1>}] \end{bmatrix} := \begin{bmatrix} \left[\mathrm{mid}\left([\dot{m}_{CG}^{<l>}]\right) \ ; \ \sup\left([\dot{m}_{CG}^{<l>}]\right)\right] \\ \left[\inf\left([\Delta\vartheta^{<l>}]\right) \ ; \ \mathrm{mid}\left([\Delta\vartheta^{<l>}]\right)\right] \end{bmatrix},$$

$$\begin{bmatrix} [\dot{m}_{CG}^{<L+2>}] \\ [\Delta\vartheta^{<L+2>}] \end{bmatrix} := \begin{bmatrix} \left[\inf\left([\dot{m}_{CG}^{<l>}]\right) \ ; \ \mathrm{mid}\left([\dot{m}_{CG}^{<l>}]\right)\right] \\ \left[\mathrm{mid}\left([\Delta\vartheta^{<l>}]\right) \ ; \ \sup\left([\Delta\vartheta^{<l>}]\right)\right] \end{bmatrix},$$

and

$$\begin{bmatrix} [\dot{m}_{CG}^{<L+3>}] \\ [\Delta\vartheta^{<L+3>}] \end{bmatrix} := \begin{bmatrix} \left[\mathrm{mid}\left([\dot{m}_{CG}^{<l>}]\right) \ ; \ \sup\left([\dot{m}_{CG}^{<l>}]\right)\right] \\ \left[\mathrm{mid}\left([\Delta\vartheta^{<l>}]\right) \ ; \ \sup\left([\Delta\vartheta^{<l>}]\right)\right] \end{bmatrix}. \tag{24}$$

All of these subintervals have to be checked for validity. The validity test is related to the sliding surface $s(t) = 0$ which is defined by the error measure introduced in Sec. III-B. Depending on the error measure $s(t)$, a valid control vector $\left[\mathbf{u}^{<l>}\right]$ can be obtained with

$$v := \begin{cases} \sup\{[v]\} < \inf\{\left[\dot{m}_{CG}^{<l>}\right] \cdot \left[\Delta\vartheta^{<l>}\right]\} & \text{for } s \geq 0 \\ \inf\{[v]\} \ > \sup\{\left[\dot{m}_{CG}^{<l>}\right] \cdot \left[\Delta\vartheta^{<l>}\right]\} & \text{for } s < 0 \ . \end{cases} \tag{25}$$

Guaranteed admissible control vectors correspond to the property of *guaranteed consistency*. These intervals are written into a list of length L. *Guaranteed inconsistent* intervals with $\sup\{[v]\} > \sup\{\left[\dot{m}_{CG}^{<l>}\right] \cdot \left[\Delta\vartheta^{<l>}\right]\}$ for $s \geq 0$ or $\inf\{[v]\} < \inf\{\left[\dot{m}_{CG}^{<l>}\right] \cdot \left[\Delta\vartheta^{<l>}\right]\}$ for $s < 0$ are deleted, whereas all other intervals are *undecided*. Thus, they are written into a list of intervals that are further subdivided with the goal to find further admissible control intervals.

Finally, the actual system input is chosen from the list of all guaranteed admissible control vectors such that it additionally minimizes the criterion

$$\begin{aligned} \left[J_k^{<l>}\right] = \kappa_1 \cdot \left(\left[\Delta\vartheta_k^{<l>}\right]\right)^2 + \kappa_2 \cdot \left(\left[\dot{m}_{CG,k}^{<l>}\right]\right)^2 + \\ \kappa_3 \cdot \left(\left[\Delta\vartheta_k^{<l>}\right] - [\Delta\vartheta_{k-1}]\right)^2 + \\ \kappa_4 \cdot \left(\left[\dot{m}_{CG,k}^{<l>}\right] - [\dot{m}_{CG,k-1}]\right)^2 \ . \end{aligned} \tag{26}$$

Choosing the minimizer $l^* = \arg\min_{l=1,\ldots,L}\{\inf\left[J_k^{<l>}\right]\}$ leads to the optimal control vector

$$\mathbf{u} := \begin{bmatrix} \mathrm{mid}\left[\dot{m}_{CG,k}^{<l^*>}\right] \\ \mathrm{mid}\left[\Delta\vartheta^{<l^*>}\right] \end{bmatrix} \tag{27}$$

that further guarantees asymptotic stability. An illustration of the consistency test is shown in Fig. 3 for the case $s > 0$. Here, the fixed actuator constraints are depicted by dotted lines. On the left-hand side, the consistency classification is displayed in the $[\dot{m}_{CG,k}]$-$[\Delta\vartheta]$-plane, where the guaranteed consistent interval boxes have to be detected. Moreover, the right-hand side shows how this procedure is applied at each discretization step t_k. Note, that the absolute control effort is quantified by choosing the parameters κ_1 and κ_2, while control variations from the time step t_{k-1} to t_k are penalized by the factors κ_3 and κ_4 in (26).

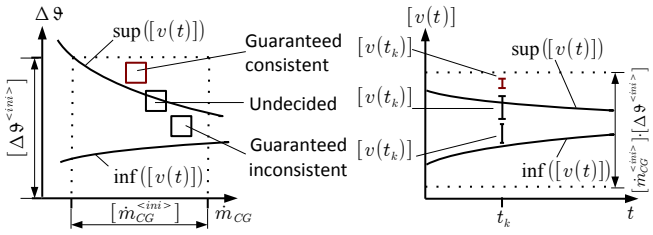

Fig. 3: Subdivision strategy.

D. Experimental Validation

The following experiment is concerned with the temperature control of the SOFC stack module during the heating phase, in which the anode gas consists of pure nitrogen N_2 with a constant mass flow. For that purpose, the control law derived above including the subdivision strategy is implemented in a C++ code using the C-XSC library [3] for basic interval computations on the corresponding real-time environment. In Fig. 4, the cathode gas mass flow $\dot{m}_{CG}$ (solid line) and the cathode gas temperature ϑ_{CG} (solid line) computed by the interval-based sliding mode control structure are depicted for the heating phase of the SOFC. According to the procedure described above, these inputs guarantee asymptotic stability. Furthermore, the predefined trajectories for the temperature ϑ_{AG} of the anode gas preheater (dashed line) and the corresponding anode gas mass flow $\dot{m}_{AG}$ (dashed line) are shown in Figs. 4(a) and 4(b).

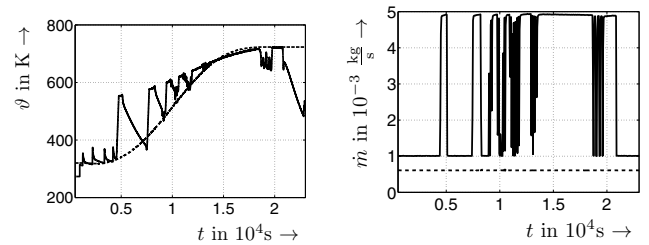

(a) Preheater temperatures of the anode gas ϑ_{AG} (dashed line) and the cathode gas ϑ_{CG} (solid line).

(b) Mass flows of the anode gas $\dot{m}_{AG}$ (dashed line) and the cathode gas $\dot{m}_{CG}$ (solid line).

Fig. 4: System inputs of the stack module during the heat-up phase.

In Fig. 5(a), the desired trajectory $\vartheta_{FC,d}$ and the measured stack temperature $\vartheta_{FC,M}$ are depicted. Heating of the SOFC starts at a temperature of $\vartheta_{FC} = 297.0\text{K}$ and stops at a temperature of $\vartheta_{FC} = 473.0\text{K}$ in a time horizon of $T_{exp} = 23,000\text{s}$. The error $e = \vartheta_{FC,d} - \vartheta_{FC,M}$ describes the deviation between these values as shown in Fig. 5(b).

The excellent tracking behavior becomes possible by the online evaluation of the interval-based sliding mode controller which exploits the disturbance estimate $\hat{d}$ of the observer for a correction of the current control signal.

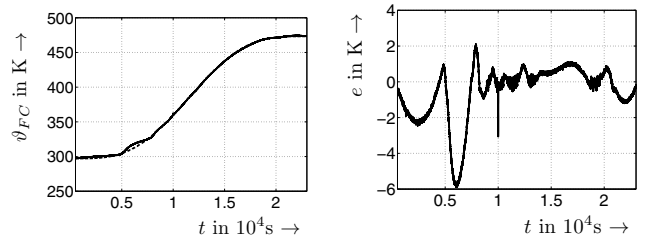

(a) Desired trajectory for the stack module temperature $\vartheta_{FC,d}$ (dashed line) and its actual time response $\vartheta_{FC,M}$ (solid line).

(b) Deviation e between the desired trajectory and the actual stack temperature.

Fig. 5: Experimental result of the disturbance observer-based interval sliding mode control procedure.

IV. Conclusion and Outlook

To stabilize uncertain dynamic systems in a guaranteed way, interval methods can be applied to account for an imperfect knowledge about the parameters of the mathematical model. For the thermal subsystem of the SOFC stack module, a control-oriented model has been derived on the basis of the first law of thermodynamics in an integral form. To account for imperfect system knowledge, interval parameters can be detected by verified optimization algorithms that enclose the true parameter values in a guaranteed way. Furthermore, uncertainty in the system model is accounted for by an interval-based sliding mode control law. This approach makes it possible to stabilize the thermal behavior of the SOFC in a guaranteed way even if uncertainties in the parameterization and external disturbances occur. The interval-based sliding mode control law stabilizes a dynamic system towards a desired trajectory on the basis of a Lyapunov function. In addition, a scalar system model has been derived for the thermal behavior of the stack module which was used as a basis for the control procedure that has been validated experimentally using C-XSC as an interval arithmetic function library on a real-time system. In this experiment, a disturbance observer has been introduced for the estimation of errors resulting from simplifications of the system model.

The task for future work is the extension of the system model to higher dimensions in order to approximate the temperature distribution in the interior of the stack module. Regarding this set of uncertain ODEs, the interval-based sliding mode control law will be employed to stabilize the thermal behavior with respect to a given time-varying temperature profile. Here, the control of flat and non-flat system outputs will be investigated. In a second task, the before-mentioned controller can be replaced or extended with an interval-based model predictive control law with the focus on a robust disturbance rejection in connection with the calculation of optimal system inputs to prevent local overtemperatures in the interior of the stack module, cf. [11].

References

[1] R. Bove and S. Ubertini, editors. *Modeling Solid Oxide Fuel Cells*. Springer, Berlin, 2008.

[2] L. Jaulin, M. Kieffer, O. Didrit, and É. Walter. *Applied Interval Analysis*. Springer–Verlag, London, 2001.

[3] W. Krämer. XSC Languages (C-XSC, PASCAL-XSC) — Scientific Computing with Validation, Arithmetic Requirements, Hardware Solution and Language Support, n.a. `http://www.math.uni-wuppertal.de/~xsc/`.

[4] Th. Dötschel, E. Auer, A. Rauh, and H. Aschemann. Thermal Behavior of High-Temperature Fuel Cells: Reliable Parameter Identification and Interval-Based Sliding Mode Control. *Soft Computing*, 2013. Available online.

[5] Th. Dötschel, A. Rauh, and H. Aschemann. Reliable Control and Disturbance Rejection for the Thermal Behavior of Solid Oxide Fuel Cell Systems. In *Proc. of MATHMOD 2012*, Vienna, Austria, 2012. To appear on `ifac-papersonline.net`.

[6] J.T. Pukrushpan, A.G. Stefanopoulou, and H. Peng. *Control of Fuel Cell Power Systems: Principles, Modeling, Analysis and Feedback Design*. Springer, Berlin, 2nd edition edition, 2005.

[7] A. Rauh and H. Aschemann. Parameter Identification and Observer-Based Control for Distributed Heating Systems – The Basis for Temperature Control of Solid Oxide Fuel Cells. *Mathematical and Computer Modelling of Dynamical Systems*, 18(4):329–353, 2012.

[8] A. Rauh, Th. Dötschel, and H. Aschemann. Experimental Parameter Identification for a Control-Oriented Model of the Thermal Behavior of High-Temperature Fuel Cells. In *CD-Proc. of IEEE Intl. Conference on Methods and Models in Automation and Robotics MMAR*, Miedzyzdroje, Poland, 2011.

[9] A. Rauh, Th. Dötschel, E. Auer, and H. Aschemann. Interval Methods for Control-Oriented Modeling of the Thermal Behavior of High-Temperature Fuel Cell Stacks. In *Proc. of 16th IFAC Symposium on System Identification SysID 2012*, Brussels, Belgium, 2012.

[10] A. Rauh, L. Senkel, and H. Aschemann. Sensitivity-Based State and Parameter Estimation for Fuel Cell Systems. In *Proc. of 7th IFAC Symposium on Robust Control Design*, Aalborg, Denmark, 2012.

[11] A. Rauh, L. Senkel, J. Kersten, and H. Aschemann. Verified Stability Analysis for Interval-Based Sliding Mode and Predictive Control Procedures with Applications to High-Temperature Fuel Cell Systems. In *Proc. of 9th IFAC Symposium on Nonlinear Control Systems*, Toulouse, France, 2013. Accpeted.

[12] Ch. Stiller, B. Thorud, O. Bolland, R. Kandepu, and L. Imsland. Control Strategy for a Solid Oxide Fuel Cell and Gas Turbine Hybrid System. *Journal of Power Sources*, 158:303–315, 2006.